Malachite Green Adsorption by Base-treated Wood Mill Residues: Kinetics, Isotherms, and Thermodynamic Studies

Ali El-Rayyes, a,b Edwin Andrew Ofudje ,c,* Akeem Adesina Bamgbade,d Moamen S. Refat, Amnah Mohammed Alsuhaibani,f James Asamu Akande,g Olajire S. Olanrele, and Nathanael Yinka Ilesanmi

The adsorption of malachite green (MG) was studied using chemically activated wood mill residues via a batch process. Maximum adsorption of 44.6 mg/g and 55.7 mg/g was obtained at optimum reaction time of 150 min and 180 min for the raw sample and the chemically treated sample, respectively. The kinetics analysis revealed that the adsorption process of MG by the raw sample is best described by a pseudo-first-order, whereas the pseudo-second-order model provided a better fit for the base-treated sample. The thermodynamic parameter of free energy confirmed the spontaneity and feasibility of the process, while positive enthalpy change (ΔH) values for both raw (17.2 kJ/mol) and treated samples (21.4 kJ/mol) affirmed that the adsorption process was endothermic. Desorption experiments demonstrated the potential for adsorbent regeneration and reusability, enhancing sustainability. Fourier transform infrared analysis confirmed that the base-modified wood residues effectively adsorbed MG dye, as evidenced by changes in key functional groups like O-H, N-H, C=C, and C-O. These findings contribute to the development of efficient adsorbents for environmental remediation, emphasizing the need for cost-effective and eco-friendly solutions.

DOI: 10.15376/biores.20.3.7378-7404

Keywords: Adsorption; Isotherms; Malachite green; Pollution; Remediation

Contact information: a: Center for Scientific Research and Entrepreneurship, Northern Border University, Arar 73213, Saudi Arabia; b: Chemistry Department, College of Science, Northern Border University, Arar, Saudi Arabia; c: Department of Chemical Sciences, Mountain Top University, Ogun State, Nigeria; d: Department of Chemistry, College of Physical Sciences, Federal University of Agriculture, Abeokuta, Ogun State, Nigeria; e: Department of Chemistry, College of Science, Taif University, P.O. Box 11099, Taif 21944, Saudi Arabia; f: Department of Sports Health, College of Sport Sciences & Physical Activity, Princess Nourah bint Abdulrahman University, P.O. Box 84428, Riyadh 11671, Saudi Arabia; g: Department of Chemistry and Biochemistry, Caleb University, Imota, Lagos State, Nigeria; * Corresponding author: eaofudje@mtu.edu.ng

INTRODUCTION

The release of synthetic dyes from industrial effluents has emerged as a major environmental concern, necessitating effective and sustainable remediation approaches. Textile and dye-laden wastewater discharged into aquatic ecosystems can significantly contribute to water pollution, posing toxicity risks to aquatic organisms and potential health hazards to humans (Ofudje *et al.* 2024; Tsoutsa *et al.* 2024; Velinov *et al.* 2024). The untreated disposal of dye-containing effluents into water bodies can lead to severe

ecological and health consequences (Pehlivan *et al.* 2020; Velinov *et al.* 2024). Dyes alter water quality by causing discoloration, which reduces light penetration and disrupts the balance of aquatic ecosystems. This imbalance adversely impacts habitats, inhibiting the growth and reproduction of aquatic flora and fauna (Pehlivan *et al.* 2020; Velinov *et al.* 2024).

Malachite green (MG), a cationic dye widely utilized in textiles, aquaculture, food, leather tanning, and paper industries, is known for its toxic effects on aquatic life and potential health hazards to humans (Srivastava et al. 2004; Abewaa et al. 2023). The MG is used in fish farms to treat fungal infections, leading to water contamination (Srivastava et al. 2004). The MG is highly toxic to fish, invertebrates, and aquatic ecosystems, causing mutations and reproductive issues, and exposure to MG has been linked to carcinogenic, mutagenic, and cytotoxic effects in humans, while persistence and bioaccumulation of MG could lead to long-term pollution in water and sediments (Adeogun et al. 2018; Abewaa et al. 2023; Jyotshana et al. 2023). The continuous presence of MG in a water body could constitute serious health and environmental risks and as such, effective control measures must be in place to eliminate and mitigate its harmful impacts.

Synthetic dyes possess complex chemical structures that make them resistant to conventional wastewater treatment methods, such as coagulation, flocculation, and sedimentation, posing challenges for their effective removal (Adeogun *et al.* 2018; Negeno *et al.* 2022; Velinov *et al.* 2024). While advanced oxidation processes, membrane filtration, and biological treatments offer improved efficiency, they are often costly and demand specialized infrastructure and expertise (Velinov *et al.* 2024). In contrast, adsorption has gained attention as a cost-effective and environmentally friendly approach for dye removal, particularly when utilizing low-cost adsorbents derived from agricultural and industrial waste materials (Fatma *et al.* 2018; Sugiarto *et al.* 2022; Velinov *et al.* 2024; Oyebola *et al.* 2025). This method is widely recognized for its affordability and ease of implementation, making it a promising approach for wastewater treatment.

Due to the high cost of commercial activated carbon, which can be largely attributed to its requirements of purity, researchers have increasingly explored costeffective alternatives for dye removal from contaminated wastewater. Various low-cost adsorbents, such as sugarcane peel waste (Ofudje et al. 2024), MgO nanocomposites, nanobentonite, and fungal immobilization on activated carbon (Hussien-Hamad 2023), have been investigated. Other promising materials include Ziziphus spina-christi seed shells (Bashanaini 2019), seashell powder (Chowdhury and Saha 2010), cow waste (El-Rayyes et al. 2025), lignin (Du et al. 2024), and Juglans nigra shell biomass (Parimelazhagan et al. 2022). Sorbents derived from lignocellulosic biomass, including wood and agricultural residues, offer a sustainable and eco-friendly alternative for industrial and environmental applications (Fatma et al. 2018; Sugiarto et al. 2022). These biomass-based materials contain diverse functional groups, such as hydroxyl, carbonyl, carboxyl, phenolic, and amide, which play a crucial role in binding pollutants, particularly cationic contaminants like MG dye (Henao-Toro et al. 2024). However, these agricultural waste exhibits limited adsorption capacity, which can be enhanced through chemical modifications.

Alkali activation using KOH or NaOH has the potential to remove hemicellulose and disrupt lignin structures, thereby exposing more cellulose microfibrils (Cerasella *et al.* 2017; Rangabhashiyam *et al.* 2018). This process results in the transformation of

neutral surface –OH and –COOH groups into deprotonated –O⁻ and –COO⁻ groups, thus enhancing the negative surface charge (Cerasella *et al.* 2017; Rangabhashiyam *et al.* 2018). These functional group modifications increase the number and strength of adsorption sites, particularly for cationic dyes such as malachite green. The alkali treatment enhances electrostatic interactions with malachite green dye molecules, thereby increasing overall adsorption efficiency.

The growing need for effective and sustainable water treatment solutions has driven researchers to explore waste materials as potential sorbent in the removal of malachite green from wastewater. The adsorption behavior of MG onto base-treated wood mill waste was examined by analyzing the isotherm, kinetics models, and thermodynamic parameters. Through repurposing sawmill waste for environmental applications, this approach not only mitigates disposal challenges but also supports the process of adding values to waste.

EXPERIMENTAL

Materials

The malachite green and other reagents used were procured from Aldrich Sigma, India, and utilized without additional purification.

Preparation of Adsorbent

The wood mill waste was first collected from a sawmill factory in Ifo, Ogun State of Nigeria, cleaned, and dried to remove any impurities or residual moisture. The dried sample was then crushed to obtained uniform particle size in the range of 60 to 80 μm . To enhance the adsorbent's properties, chemical activation method was employed in which one part was treated with 0.5M of KOH and left for 24 h. The chemically activated samples were then removed from the base solution and filtered. Thereafter, the samples were thoroughly washed with distilled water and oven drying at 100 °C for 3 h. The activated samples were used for the experiment and further characterization. The prepared adsorbent was labeled as BTWMW, while the other portion which was not chemically treated was called RWMW.

Characterization

The obtained sorbent was subjected to structural investigation using some techniques to explore their physical and chemical nature, which are essential for evaluating adsorption efficiency. Fourier Transform Infrared (FT-IR) spectroscopy (CARY630 NBY, Thermo Fisher Scientific Instrument, Waltham, MA, USA) was used to determine the functional groups, while a Thermo Fisher Scientific, Scanning Electron Microscope (SEM) (Phenom ProX, USA) was employed to examine surface morphology and porosity. Brunauer–Emmett–Teller (BET) analysis provided insights into pore size and surface area. Additionally, the bulk density, pore size, pore volume, and surface area of the sawmill wood waste were measured using a Quantachrome NOVA 2200C (USA), while the zero-point charge (pHzPC) of the adsorbent was determined using a Zetasizer Nano ZS analyzer (Malvern, UK). The thermal property of the adsorbent was assessed using a thermogravimetric analyzer (TGA 4000, Perkin Elmer, Haarlem, Netherlands).

Adsorption Studies

The adsorption capacity of sawmill wood for malachite green dye was determined *via* batch adsorption experiments. A 15 mg portion of the adsorbent was added to aqueous solutions of malachite green in multiple conical flasks, with the pH of each solution adjusted to the optimal level using either HCl or NaOH. The mixtures were agitated at a constant speed of 150 rpm on an orbital shaker at 25 °C to ensure uniform mixing. At specific time intervals, small aliquots were extracted and analyzed using UV-Visible Spectrophotometry (Shimadzu UV-3600 UV-Vis-NIR). Key parameters, including initial concentration, wood dosage, contact time, temperature and pH, were varied to assess their influence on adsorption capacity. The amount of dye removed, and the percentage removal were evaluated using Eqs. 1 and 2,

Amount adsorbed,
$$Q_e = \frac{C_o - C_e}{m}V$$
 (1)

Percentage Removal,
$$%Q_e = \frac{C_o - C_e}{C_o} x 100$$
 (2)

where q_e (mg/g), C_0 (mg/L), C_e (mg/L), m (mg), and V (L) represent the adsorption capacity, initial and equilibrium concentrations of the adsorbate, mass of the adsorbate and volume of adsorbate used, respectively.

Regeneration Studies

Regeneration experiments were conducted to evaluate the reusability of sawmill wood as an adsorbent. After each adsorption cycle, 0.5 M of acetic acid was used to desorb the adsorbed material. The adsorbent was then washed and reused in subsequent cycles to assess its long-term stability and cost-effectiveness. The mixture was separated, and the filtrate was analyzed using a UV-Vis spectrophotometer (Shimadzu UV-3600 UV-Vis-NIR). This process was done in five cycles and the percentage desorption (PD) was calculated using Eq. 3 below,

$$PD(\%) = \frac{AD}{AA}X100\tag{3}$$

where AD represents the amount of the pollutant (mg) desorbed, and AA represents pollutant adsorbed amount (mg). All experiments were done in triplicate, and the average values recorded.

RESULTS AND DISCUSSION

MG Concentration and Contact Time Analysis

The role played using different concentrations of the pollutant as well as different reaction times was examined, as presented in Figs. 1 and 2. It was observed that adsorption increased rapidly from 30 to 120 min, indicating that active adsorption sites were readily available and malachite green molecules were being captured efficiently. This rapid increase suggests a strong initial interaction between raw wood mill waste and the dye molecules due to sufficient occupied site of adsorption. As time progresses, the rate of adsorption slows down, and equilibrium was reached around 150 to 180 min, where adsorption values remain nearly constant. This plateau indicates that most of the

available adsorption sites were occupied, and further adsorption is limited by the availability of free sites on the adsorbent. Maximal sorption of 44.6 mg/g and 55.7 mg/g was obtained at optimum reaction time of 150 min and 180 min for the raw sample and the chemically treated sample, respectively. A slight decrease in adsorption capacity at extended contact times (*e.g.*, at 200 min for the 120 mg/L solution) was observed, which could be attributed to desorption effects or minor fluctuations around the equilibrium state. Some studies have documented a rapid initial phase of adsorption, followed by a gradual decline in rate as equilibrium is approached, consistent with the observed trends. For example, research on malachite green adsorption using rattan sawdust by Hameed and El-Khaiary (2008) identified two distinct phases: an initial rapid uptake due to an abundance in active sites, followed by a slower phase as these sites became occupied, ultimately leading to equilibrium with an uptake of 62.7 mg/g. Likewise, a study on malachite green adsorption using poplar sawdust activated carbon by Yıldız *et al.* (2023) recorded an optimal uptake capacity of 150 mg/g with equilibrium achieved within 6 h.

On the impact of MG concentration, the data clearly showed that higher MG concentrations caused higher adsorption. For example, at 120 min, adsorption was 7.7 mg/g and 8.5 mg/g at MG concentration of 20 mg/L but 35.5 mg/g and 47.1 mg/g for 120 mg/L for raw and chemically-treated samples, respectively. This trend occurred because higher dye concentrations provided more molecules in solution, increasing the driving force for diffusion and adsorption onto the wood mill waste. At equilibrium (180 to 240 min), adsorption stabilized, with higher initial concentrations still maintaining greater adsorption capacities. However, the difference between adsorption at 180 and 240 min was minimal, indicating that the system had reached its maximum capacity for removal at each concentration level. The effect of initial MG concentration on adsorption capacity has been investigated in several studies, demonstrating that higher initial dye concentrations lead to increased adsorption values. This development is attributed to the greater availability of molecules of the dye in solution, which enhances the driving force for diffusion and subsequent adsorption onto the adsorbent material. For example, a study on the uptake of MG by Eucalyptus wood biochar reported by Singh et al. (2016) showed that increasing dye concentration from 25 mg/L to 100 mg/L caused a rise in uptake capacity from 20.9 mg/g to 75.5 mg/g, respectively, which was due to higher availability of molecules of the dye, which enhanced the driving force for diffusion and subsequent adsorption onto the adsorbent material.

Similarly, research on MG adsorption using rice husks by Muinde *et al.* (2017) showed that the removal efficiency of dye was reduced with increasing initial dye concentrations, suggesting that higher concentrations provide more molecules in solution, thereby increasing the driving force for diffusion and adsorption onto the adsorbent. The base-treated wood mill waste consistently showed higher adsorption capacities at all concentrations compared to the raw wood mill waste. The difference between treated and untreated samples was more noticeable at higher initial concentrations. For 120 mg/L, the treated sample achieved 55.2 mg/g, compared with 46.3 mg/g in the untreated sample. Alkaline treatments are known to modify the physicochemical properties of lignocellulosic adsorbents such as wood waste. The treatment primarily disrupts the lignin and hemicellulose structures, leading to the removal of amorphous components. As a result, the surface area and porosity of the adsorbent increase, which improves the accessibility of active binding sites for dye molecules.

Chemically, base treatment alters the surface functional groups of the adsorbent as the adsorbent surface become deprotonated, forming negatively charged sites such as $-\mathrm{O}^-$

(in the case of phenolic groups at pH > 9) and -COO⁻. The interaction mechanism between malachite green (a cationic dye) and the base-treated adsorbent is primarily governed by electrostatic attraction. The positively charged dye molecules are strongly attracted to the negatively charged functional groups introduced or exposed by the alkaline treatment. These combined structural and chemical enhancements explain the improved adsorption efficiency observed for base-treated wood waste.

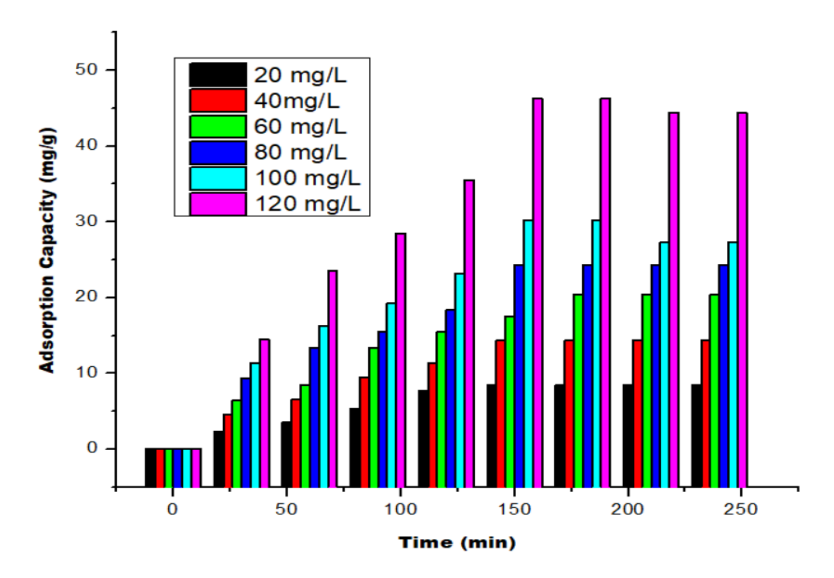


Fig. 1. Plots of contact time and initial MG concentrations for the adsorption by RWMW

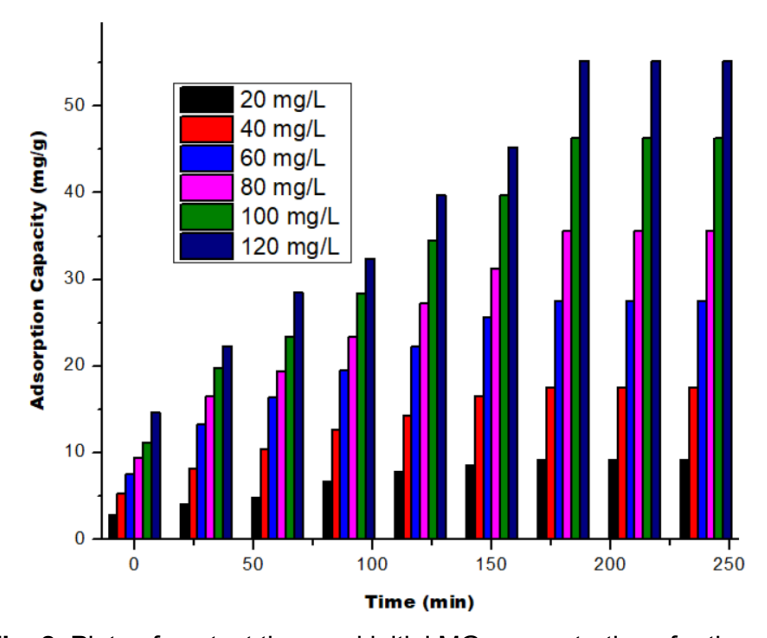


Fig. 2. Plots of contact time and initial MG concentrations for the adsorption by BTWMW

Effect of pH on the Adsorption of MG

The uptake of MG by RWMW and BTWMW is strongly influenced by pH, as it alters both the ionization state of the pollutant and the adsorbent surface charge (Fig. 3). At pH 2 and 3, the adsorption capacity was relatively low for both adsorbents (54.1% for RWMW and 57.4% for BTWMW at pH 2; 56.4% for RWMW and 63.8% for BTWMW

at pH 3). This is likely due to surface protonation at these low pH values, causing electrostatic repulsion between the adsorbent surface and the cationic malachite green dye (Muinde *et al.* 2017; Ofudje *et al.* 2020a). However, the base-treated wood mill waste showed slightly higher adsorption compared to RWMW. This was likely due to additional functional groups introduced by the base treatment, increasing the available active sites of adsorption. At pH 4 and 5, greater increase in adsorption was observed (65.3% for RWMW and 71.7% for BTWMW at pH 4; 74.7% for RWMW and 78.4% for BTWMW at pH 5). The point of zero charge (PZC) for RWMW was 4.25, while for BTWMW, it was 4.71. This means that at pH values below these points, the adsorbents surface would be positive, causing repulsion with the MG molecules that are positively charged (Ofudje *et al.* 2024; Oyebola *et al.* 2025).

Conversely, at pH greater than the PZC, the adsorbent surfaces become negative, enhancing electrostatic interaction between the dye and sorbent. Because these pH values are just above the PZC, the adsorbent surfaces start to acquire negative charges, which enhances electrostatic attraction between the adsorbent and malachite green molecules. The effect is more pronounced for BTWMW due to its higher PZC (4.71) and improved surface properties from base treatment. At pH 6, the highest adsorption capacity was recorded at this pH: 76.5% for RWMW and 86.4% for BTWMW. At this pH, the adsorbent surfaces are fully negatively charged, maximizing electrostatic attraction with malachite green. The base-treated wood mill residue demonstrated greater adsorption efficiency compared to RWMW, suggesting that base treatment enhances surface functionality, pore structure, and active site availability. At pH 8, adsorption declined, with 54.3% for RWMW and 58.4% for BTWMW. This reduction in adsorption was attributed to a rivalry between hydroxyl ions (OH-) and malachite green cations towards the sites of adsorption (Ofudje et al. 2020b; Oyebola et al. 2025). Additionally, at high pH, malachite green molecules may undergo structural changes, reducing their affinity for the adsorbent (Hameed and El-Khaiary 2008). Base treatment enhances adsorption across all pH values, with BTWMW consistently showing better sorption ability than RWMW. This improvement is because of enhanced porosity, functional groups, and surface charge properties introduced by base treatment.

Muinde et al. (2017) investigated the role played by pH on the sorption of MG dye by rice husks adsorbent. Results indicated an increased in the amount of MG removed with rise in pH, reaching an optimal value at pH 7. Beyond pH 7, the adsorption efficiency decreased. The reduced adsorption at lower pH levels (3 to 6) was attributed to the excess hydrogen ions in the solution, which contend with positive MG molecules for active sites of the rice husks, leading to decreased dye uptake. At higher pH values (8 to 9), the decline in sorption efficiency was caused by the formation of soluble hydroxyl complexes, which reduces the availability of the dye for adsorption. Similarly, the study by Oyelude et al. (2018) noted that the capacity of adsorption of pulverized teak leaf litter for MG was significantly impacted by the solution pH and that optimal removal of MG per gram of pulverized teak leaf litter occurred at a dosage of 2 g/L and within a pH range of 6 to 8. This implies that the process of sorption is more efficient with neutral pH to slightly alkaline conditions. EL-Shimaa et al. (2021) observed a similar trend when they investigated the uptake of MG by low-cost adsorbent from wastewater.

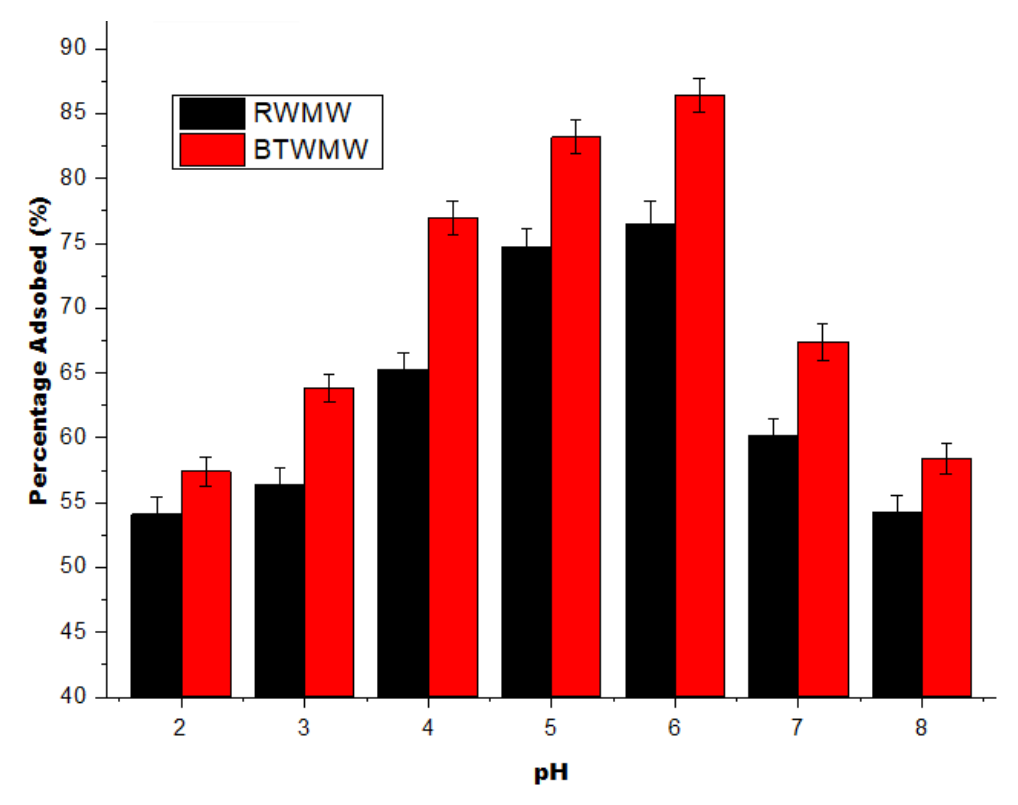


Fig. 3. Effect of pH on the sorption of MG by RWMW and BTWMW

Effect of Adsorbent Dosage

Malachite green adsorption onto RWMW and BTWMW is greatly affected by the adsorbent dosage, as a higher mass means more active sites for dye uptake, as illustrated in Fig. 4. At a low dosage of 10 mg, the adsorption percentages for RWMW and BTWMW were 53.8% and 57.3%, respectively. As the dosage increased to 15 and 20 mg, the adsorption efficiency increased notably, reaching 65.8% for RWMW and 75.5% for BTWMW. This increase is expected because a greater adsorbent dosage offers more binding sites, enhancing dye removal efficiency (Bharathi and Ramesh 2013; Ofudje et al. 2020a). At 25 mg, the highest sorption capacity was noticed for both RWMW (75.0%) and BTWMW (83.7%). At 35 mg, adsorption decreased to 69.1% for RWMW and 78.4% for BTWMW, respectively. The decline in sorption capacity at higher dosages could be a result of the adsorbent particle aggregation, which reduces the active sites and surface area for malachite green adsorption (Ofudje et al. 2024). Another possible reason is the saturation of available dye molecules in the solution, leading to no significant increase in adsorption despite the additional adsorbent (Oyelude et al. 2018; Uzosike et al. 2022). The BTWMW consistently exhibited higher adsorption capacities than RWMW across all dosages. This improvement is due to the chemical modification process, which enhances surface functional groups, increases surface area, and improves the availability of active adsorption sites.

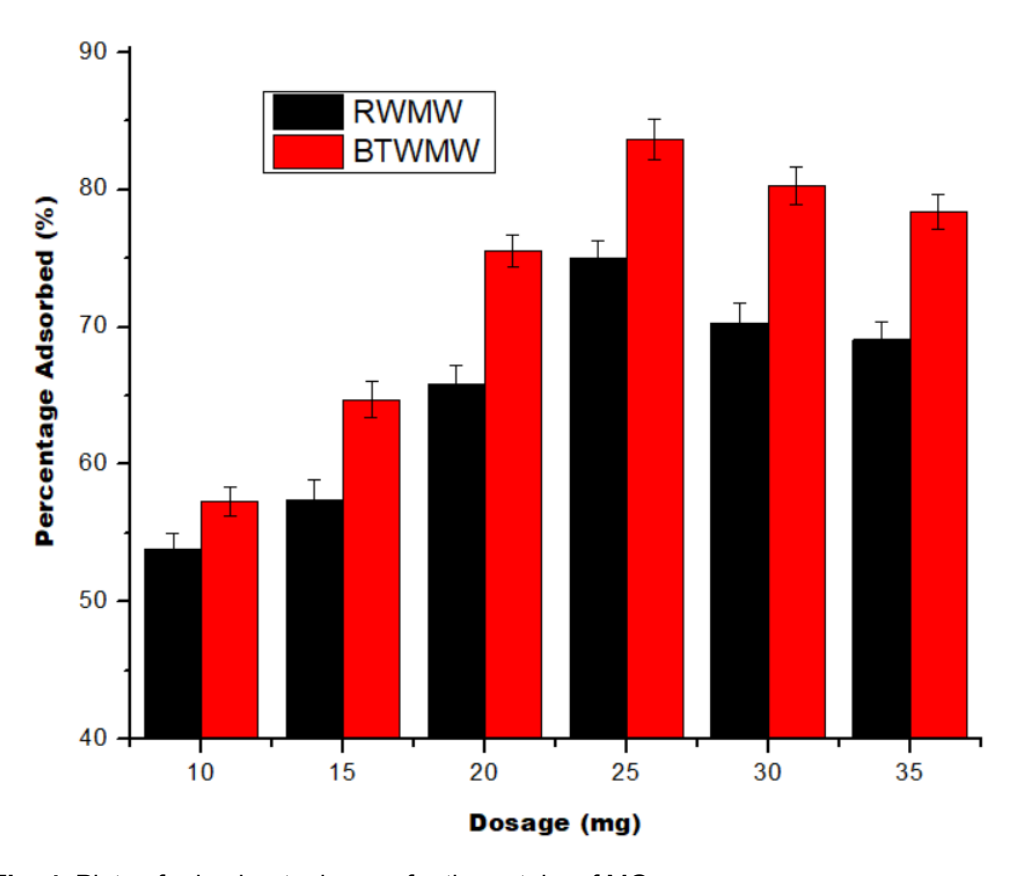


Fig. 4. Plots of adsorbents dosage for the uptake of MG

Pseudo-First-Order Kinetics

This model is commonly used to describe the adsorption process of solutes onto solid adsorbents. It can be expressed as Eq. 4 (Lagergren 1898; Blanchard *et al.* 1984; Bharathi and Ramesh 2013; Oyelude *et al.* 2018; Oyebola *et al.* 2025),

$$\log(Q_e - Q_t) = \log Q_e - \frac{k_1}{2.303}t \tag{4}$$

where Q_t denotes the adsorbed amount at time t (mg/g), k_1 stands for the pseudo-first-order rate constant (min⁻¹), and t is time (min). The parameters were estimated by plotting $\log(Q_e-Q_t)$ against t, as shown in Fig. 5. The corresponding values are presented in Tables 1 and 2. The data provides insights into the adsorption mechanism and the best-fitting kinetic model. In case of the raw data, the calculated adsorption capacities ($Q_e(cal)$) were close to the experimental values ($Q_e(exp)$), with high R² values (0.991 to 0.998), indicating a good fit. The % RMSE (root mean squared errors) values were also low (0.009 to 0.044), suggesting a reasonable agreement with the first-order model. For base-treated wood mill waste, the first-order rate constant (k_1) values ranged from 0.04 to 0.82, with R² values (0.968 to 0.996) showing a strong correlation. The % RMSE values were relatively small (0.010 to 0.072), indicating that the first-order model fits well.

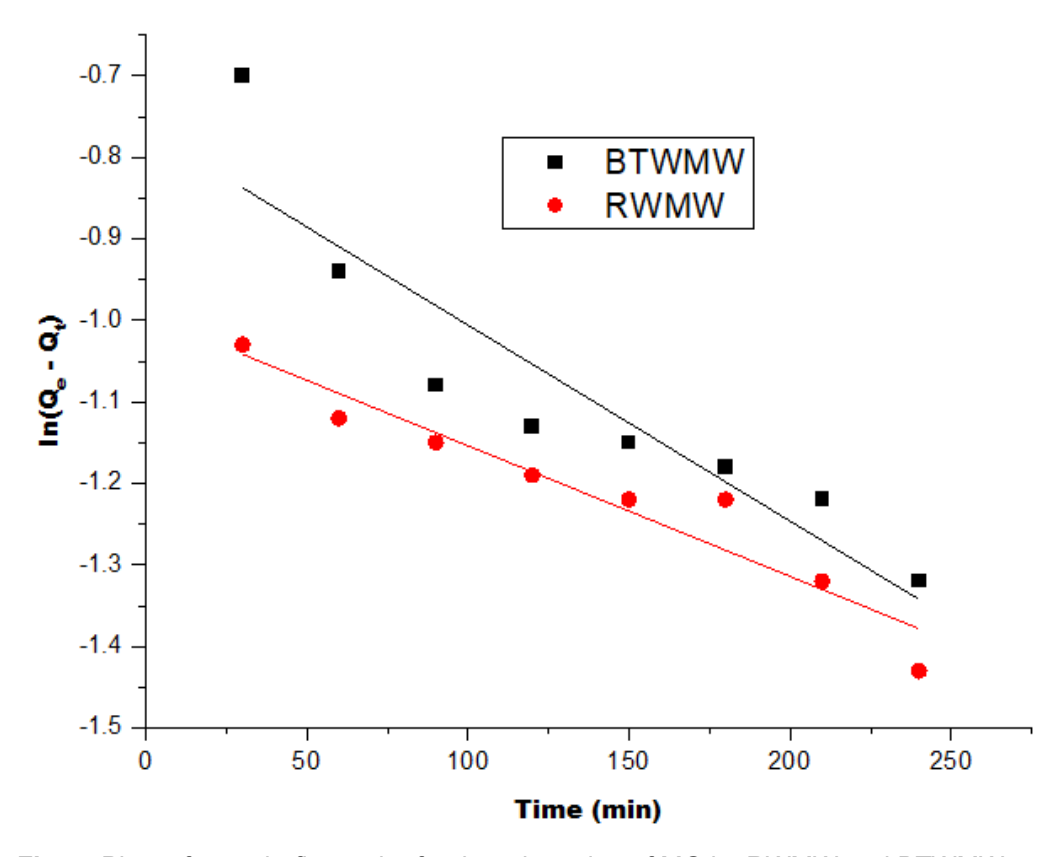


Fig. 5. Plots of pseudo-first-order for the adsorption of MG by RWMW and BTWMW

Pseudo-Second-Order Kinetics

The model can be expressed as follows (Ho and McKay 1999; Ho 2006; Bharathi and Ramesh 2013; Oyelude *et al.* 2018; Oyebola *et al.* 2025),

$${}^{t}\!\!/\!\!Q_{t} = {}^{1}\!\!/\!\!k_{2} Q_{t} + {}^{t}\!\!/\!\!Q_{e} \tag{5}$$

where Q_t and Q_e are as defined previously, k_2 is the rate constant (g/mg·min) for the pseudo-second-order equation. The plots of t/Q_t versus t is shown in Fig. 6, and Tables 1 and 2 contained the parameters so computed. The best fit was ascertained using root mean square errors (Adeogun *et al.* 2018):

$$RMSE = \sqrt{\frac{\sum_{i}^{N} (Q_{(exp)} - Q_{(cal)})^{2}}{N}}$$
(6)

For the raw sample, the R^2 values were consistently high (0.977 to 0.997), showing a strong correlation, but the % RMSE values (0.030 to 0.124) were slightly higher than those of the first-order model, indicating that while this model provided a good fit, the first-order model performed slightly better in predicting adsorption at lower concentrations. For base-treated wood mill waste, the second-order rate constant (k_2) values ranged from 0.036 to 0.103, with R^2 values (0.978 to 0.997), showing a very strong correlation. The % RMSE values were significantly lower (0.000 to 0.022) compared to the first-order model, indicating that pseudo-second-order kinetics provides

a better fit. Compared to raw wood mill waste, the k_2 values for base-treated waste were higher, suggesting an increased rate of adsorption. The $Q_{\rm e(cal)}$ values were also closer to $Q_{\rm e(exp)}$ in this model, reinforcing the conclusion that pseudo-second-order kinetics dominates adsorption on base-treated waste (Ho and McKay 1999).

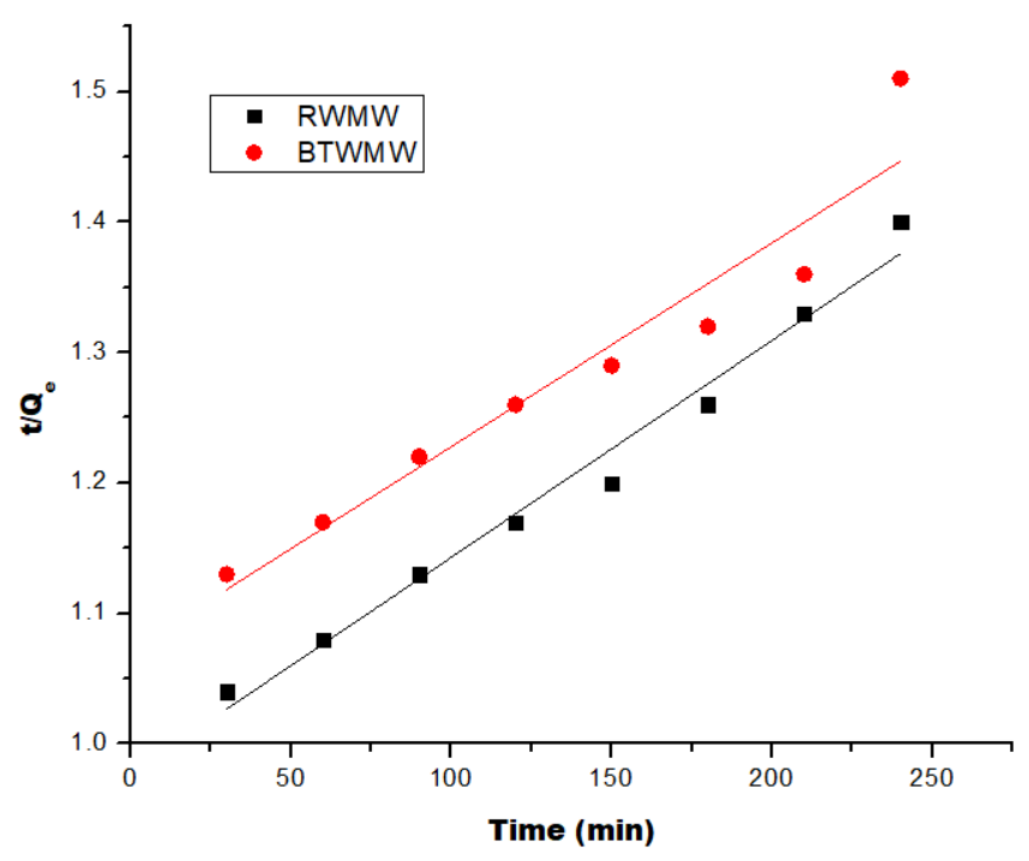


Fig. 6. Plots of pseudo-second-order for the uptake of MG by RWMW and BTWMW

Intraparticle Diffusion Model (IDM)

The IDM is widely used to describe adsorption when pore diffusion significantly influences the adsorption rate. This model helps identify whether the process is governed by film diffusion, intraparticle diffusion, or the collection of both. It is mathematically represented as Eq. 7 (Adeogun *et al.* 2018; Uzosike *et al.* 2022),

$$Q_t = k_p t^{1/2} + C_i \tag{7}$$

where k_p represents intra-particle diffusion rate constant (mg/g/min^{1/2}), and C_i denotes boundary layer thickness. When Q_t was plotted against $t^{1/2}$ as revealed in Fig. 7, the parameters given in Tables 1 and 2 were obtained.

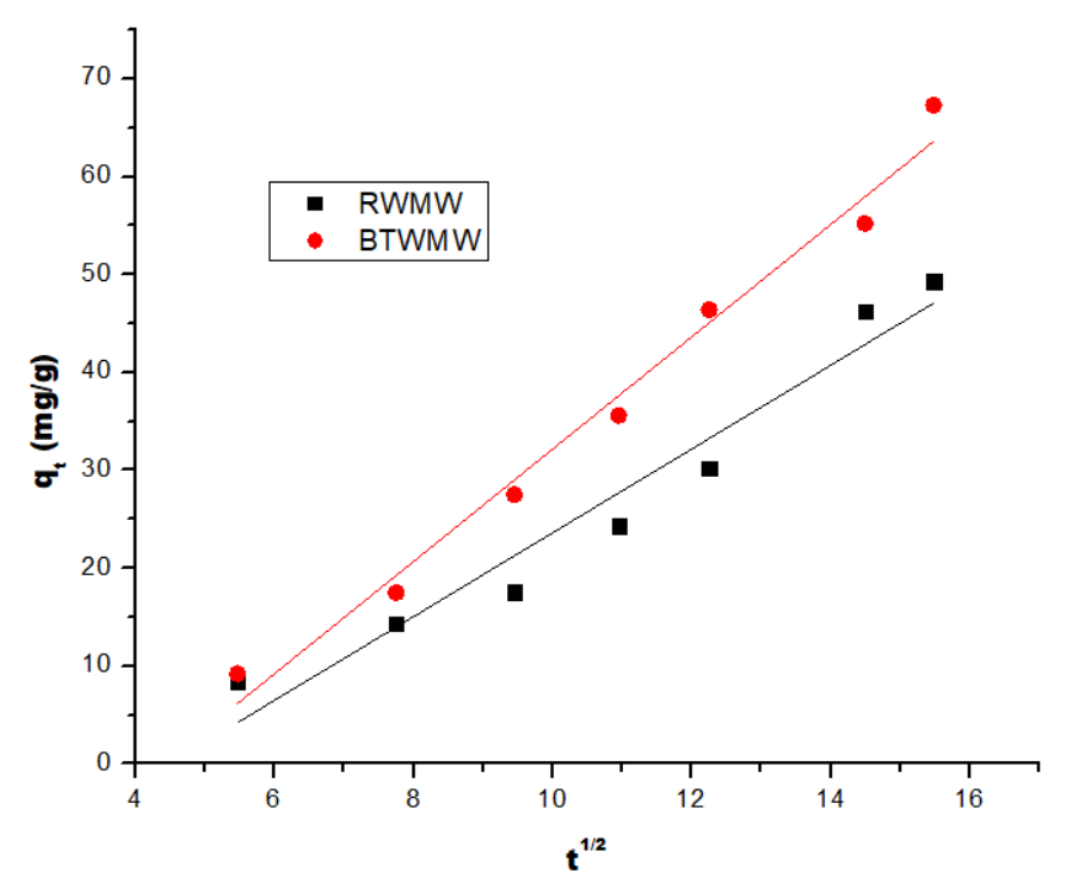


Fig. 7. The IDM plots for the uptake of MG by RWMW and BTWMW

For the untreated sample, the high R^2 values (0.988 to 0.998) indicate that diffusion played a significant role in adsorption. The K_p values (2.801 to 12.101 (mg/g/min^{1/2})) increased with concentration, suggesting that diffusion resistance decreased as concentration increased, making the process more efficient. The C_i values (0.358 to 3.958 mg/g) indicate boundary layer effects, meaning surface adsorption was also occurring slowly enough to affect the overall rate, along with intra-particle diffusion. For base-treated waste, the K_p values (1.48 to 11.3 (mg/g/min^{1/2})) and C_i values (1.92 to 13.1 mg/g) increased with concentration, showing that diffusion resistance decreased as adsorption progresses. The R^2 values (0.988 to 0.998) indicate a strong correlation. When compared to raw wood mill waste, the values of K_p were higher for base-treated adsorbent, suggesting improved intra-particle diffusion. The higher C values indicate a more significant boundary layer effect, meaning surface adsorption also played a major role in limiting the rate of adsorption.

In summary, for RWMW, the pseudo-first-order model provided the best fit, as indicated by high coefficients of determination ($R^2 = 0.991-0.998$), low RMSE values, and good agreement between experimental and calculated adsorption capacities. Conversely, for the chemically treated sample (BTWMW), the pseudo-second-order model yielded the highest R^2 values (up to 0.997), the lowest RMSE values (0.001 to 0.022), and closer agreement between experimental and theoretical q_e values. The intraparticle diffusion model indicated a multi-step process in both cases, with higher

7389

diffusion rate constants (K_p) and boundary layer effects observed in BTWMW, implying enhanced pore diffusion and surface complexity after treatment.

Table 1. Kinetics Studies of MG Adsorption by RWMW

	C₀ (mg/L)	20 mg/L	40 mg/L	60 mg/L	80 mg/L	100 mg/L	120 mg/L
	Q _e (exp) (mg/g)	8.400	14.300	17.540	24.300	30.200	46.300
order	Q _e (cal) (mg/g)	9.24	16.37	19.14	25.26	31.12	48.78
it o	<i>k</i> ₁ (min ⁻¹)	0.020	0.016	0.013	0.016	0.017	0.013
First	R ²	0.998	0.996	0.994	0.998	0.996	0.991
	% SSE	0.030	0.044	0.028	0.012	0.009	0.016
_	Q _e (cal) (mg/g)	11.85	18.93	20.86	29.93	34.91	50.92
Second	k ₂ (g/mg/min)	0.025	0.038	0.053	0.059	0.071	0.085
Sec	\mathbb{R}^2	0.988	0.996	0.993	0.997	0.977	0.992
	% SSE	0.124	0.098	0.057	0.070	0.047	0.030
Intra particle diffusion	K_p (mg/g/min ^{1/2})	2.801	3.362	5.011	7.706	9.320	12.101
	C _i (mg/g)	0.787	0.358	3.958	1.223	1.143	0.748
	R^2	0.988	0.994	0.989	0.997	0.995	0.988

Table 2. Kinetics Studies of MG Adsorption by BTWMW

	C₀ (mg/L)	20 mg/L	40 mg/L	60 mg/L	80 mg/L	100 mg/L	120 mg/L
First order	Q _e (exp) (mg/g)	9.200	17.500	27.500	35.600	46.400	55.200
	Q₅ (cal) (mg/g)	6.99	20.35	30.86	34.078	44.91	58.12
irst	<i>k</i> ₁ (min ⁻¹)	0.04	0.73	0.82	0.09	0.110	0.150
ш	R ²	0.968	0.996	0.974	0.988	0.996	0.996
	% SSE	0.072	0.049	0.037	0.013	0.010	0.016
-	Q _e (cal)	9.86	16.86	26.73	36.37	47.33	54.93
Second	k ₂ (g/mg/min)	0.036	0.056	0.061	0.071	0.086	0.103
Sec	R ²	0.996	0.995	0.993	0.988	0.978	0.997
	% SSE	0.022	0.011	0.008	0.007	0.001	0.001
∞ =	K_p (mg/g/min ^{1/2})	1.48	3.717	5.264	7.074	8.345	11.289
Intra particle diffusion	C (mg/g)	1.925	3.044	6.894	9.159	10.586	13.142
Pa pa	R ²	0.996	0.994	0.988	0.994	0.989	0.998

Langmuir Isotherm Analysis

The Langmuir isotherm describes adsorption taking place on a homogenous surface with finite active adsorption sites and it can be represented thus (Adeogun *et al.* 2018; Oyelude *et al.* 2018; Shanmugarajah *et al.* 2018; Ofudje *et al.* 2024):

$$\frac{C_e}{q_e} = \frac{1}{K_L q_m} + \frac{C_e}{q_m} \tag{8}$$

The separation factor (R_L) expression that could be use to predict the favorability of adsorption is given as (Adeogun *et al.* 2018),

$$R_L = \frac{1}{(1 + K_L C_o)} \tag{9}$$

where the maximum sorption capacity is given as Q_{max} (mg/g), and $K_{\text{L}}(\text{L/mg})$ is the Langmuir constant. The graph representing this model is shown in Fig. 8 and Table 3 contains the constants values. The Q_{max} was obtained as 49.1 and 61.0 mg/g for raw and chemically treated sample, respectively, indicating the highest amount of malachite green that can be adsorbed.

The separation factor (R_L) was 0.298 and 0.021 for raw and modified sample, which falls within the range $0 < R_L < 1$, confirming that adsorption was favorable (Ofudje et al. 2024). A lower R_L value suggests stronger adsorption, and with this drastic reduction for treated sample, suggests that base treatment improves the attraction of the sorbent towards malachite green, making the sorption more favorable.

The R² for the Langmuir model was 0.987 for the treated sample, which was higher than the 0.788 observed for raw wood mill waste. This confirms that the adsorption process followed a monolayer adsorption mechanism, with no significant interaction amount sites of adsorption, and base treatment further enhanced the fit of the Langmuir model.

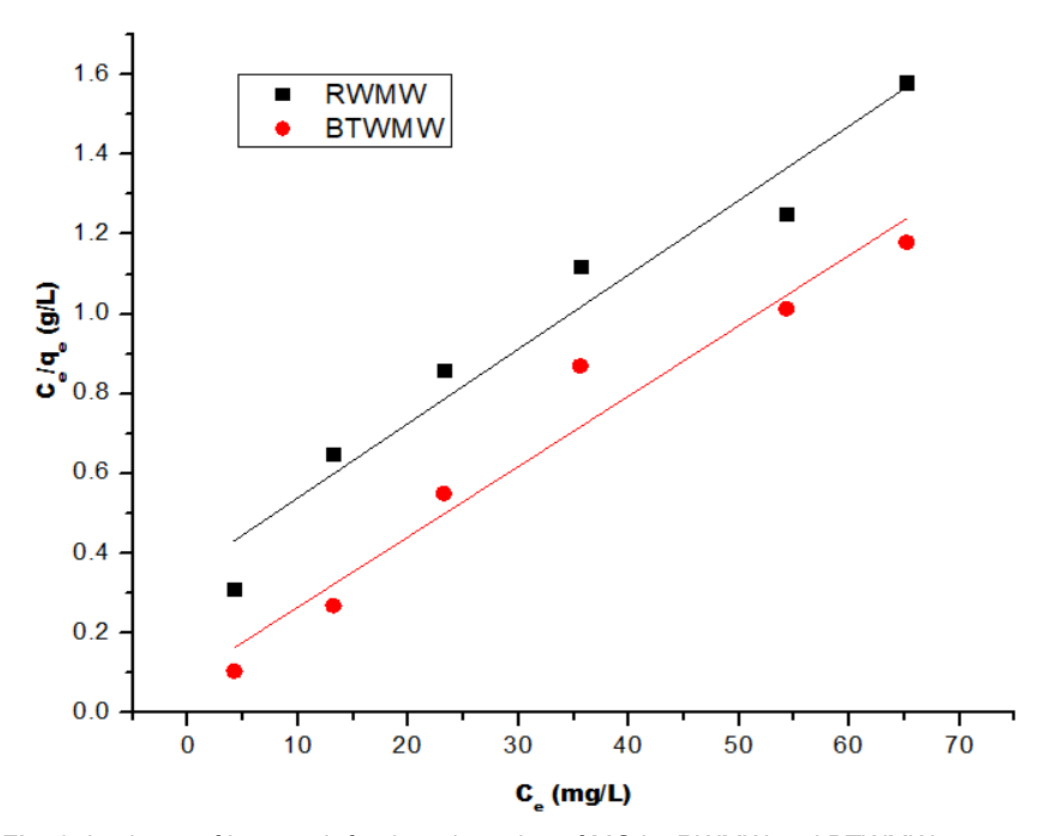


Fig. 8. Isotherm of Langmuir for the adsorption of MG by RWMW and BTWMW

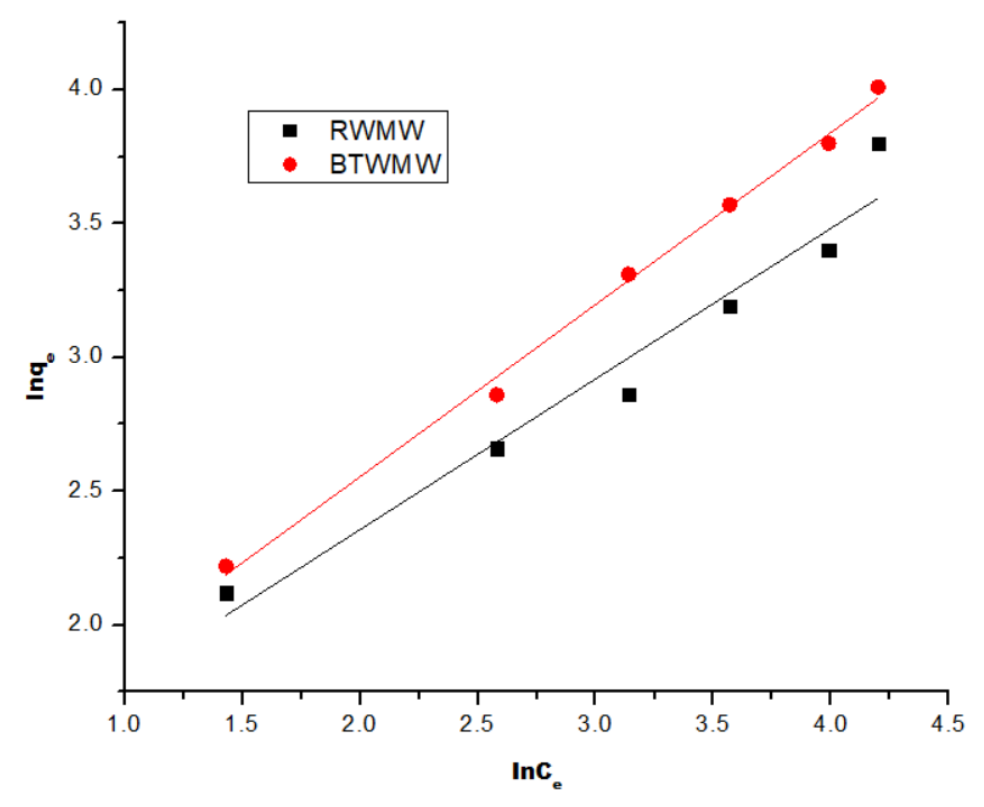


Fig. 9. Isotherm of Freundlich for the adsorption of MG by RWMW and BTWMW

Freundlich Isotherm Analysis

This isotherm can be deployed to explain adsorption occurring on a heterogeneous surface with sorption sites having different energy levels. The model can be expressed mathematically as (Muinde *et al.* 2017; Adeogun *et al.* 2018):

$$Inq_e = InK_F + \frac{1}{n}C_e \tag{10}$$

The Freundlich constant is given as K_F (mg/g), which defines capacity of adsorption, and n represents the intensity of adsorption. The uptake process is said to be favorable when 1/n is smaller than 1. The graph representing this model is provided in Fig. 9, and all obtained constants are listed in Table 3. The Freundlich constant (K_F), which represents adsorption capacity, was 46.9 (mg/g)(mg/L)^{-1/2}, which was higher than the 34.6 (mg/g)(mg/L)^{-1/2} observed for raw wood mill waste. This further indicates that base treatment enhanced adsorption efficiency. The adsorption intensity parameter (1/n) was 0.025, much lower than the 0.315 recorded for raw wood mill waste. Because 0 < 1/n < 1 indicates favorable adsorption, the lower value suggests that the adsorption sites on the base-treated adsorbent had a much stronger affinity for malachite green. The coefficient of determination (R^2) for the Freundlich model was 0.998, higher than the Langmuir model's 0.987, but since the R^2 values for both models are high enough (greater than 0.9), it is not possible to reject either one of them suggesting cooperative adsorption process.

	Parameters	RWMW	BTWMW
Langmuir	Q _{max} (mg/g)	49.14	61.038
	R∟	0.298	0.021
	R ²	0.788	0.987
Freundlich	K _F (mg/g)(mg/L) ^{-1/2}	34.57	46.921
	1/n	0.315	0.025
	R ²	0.984	0.998

Table 3. Isotherms Values for the Sorption of MG by RWMW and BTWMW

Table 4 showcases published results for the performance of some adsorbents in removing MG. The studied adsorbents gave high adsorption capacities of 49.1 mg/g for the raw sample and 61.0 mg/g for the chemically treated sample, outperforming many alternative materials. This comparison underscores the potential of wood waste as an effective, cost-efficient, eco-friendly, and sustainable solution for treating malachite green and cadmium ion pollutants in wastewater.

Table 4. Various Adsorbents and their for the Adsorption of MG by RWMW and BTWMW

Adsorbents	Q _{max}	References
	(mg/g)	
MgO impregnated clay	17.2	Hussien-Hamad (2023)
Nano-bentonite	13.8	Hussien-Hamad (2023)
Seashell powder	42.3	Chowdhury and Saha (2010)
Shells seeds of Ziziphus spina-christi	48.7	Bashanaini (2019)
Juglans nigra shell biomass	54.4	Parimelazhagan <i>et al</i> . (2022
Rice husks	6.5	Muinde <i>et al</i> . (2017)
Catha edulis	5.62	Abate <i>et al.</i> (2020)
Salacca zalacca	69.44	Hasanah <i>et al.</i> (2023)
Acid functionalized maize cob	64.52	Ojediran <i>et al</i> . (2021)
Pyracantha coccinea M. J. Roemer plant	117.745	Deniz, (2024)
Carbonized pomegranate peel	31.45	Gunduz and Bayrak (2017)
Chinese fan palm fruit biochar	21.41	Giri <i>et al</i> . (2022)
Nano-magnetic Bauhinia variagata fruit	30.1	Bayram <i>et al</i> . (2022)
RWMW	49.14	This study
BTWMW	61.038	This study

Temperature Effect and Thermodynamic Evaluations

The data presented in Fig. 10 shows the role of temperature on the adsorption of malachite green dye by RWMW and BTWMW adsorbents. For RWMW, adsorption capacity increased from 51.5% at 25 °C to 75.3% at 45 °C, whereas for BTWMW, the adsorption percentage increases from 57.3% at 25 °C to 82.4% at 40 °C. This suggests that higher temperatures enhanced dye adsorption. At 45 °C, RWMW reached its maximum adsorption capacity, but further increasing the temperature to 55 °C led to a slight decrease (71.3%). Similarly, BTWMW reached its maximum adsorption at 40 °C and thereafter it showed a slight decline to 74.5% at 55 °C. This suggests that beyond a

7393

certain temperature, desorption or decreased adsorption efficiency occurred, possibly due to the weakening of dye-adsorbent interactions or expansion of the adsorbent pores, which may release some previously adsorbed molecules. The reduction indicates that at higher temperatures, desorption or weakened interactions may occur (Guruprasad *et al.* 2024).

Variables of thermodynamic like Gibbs free energy (ΔG), enthalpy (ΔH), and entropy (ΔS) provide insights into the feasibility, spontaneity, and nature of adsorption processes (Ofudje *et al.* 2024; Oyebola *et al.* 2025). The data for raw wood mill waste (RWMW) and base-treated wood mill waste (BTWMW) revealed differences in adsorption behavior, highlighting the impact of base treatment on adsorption thermodynamics. These parameters were computed following Eqs. 11 to 13 (Konicki *et al.* 2017; Hussien-Hamad 2023; Oyebola *et al.* 2025):

$$K_d = \frac{q_e}{C_e} \tag{11}$$

$$\ln K_d = \frac{\Delta S^o}{R} - \frac{\Delta H^o}{RT} \tag{12}$$

$$\Delta G^o = RTInK_d \tag{13}$$

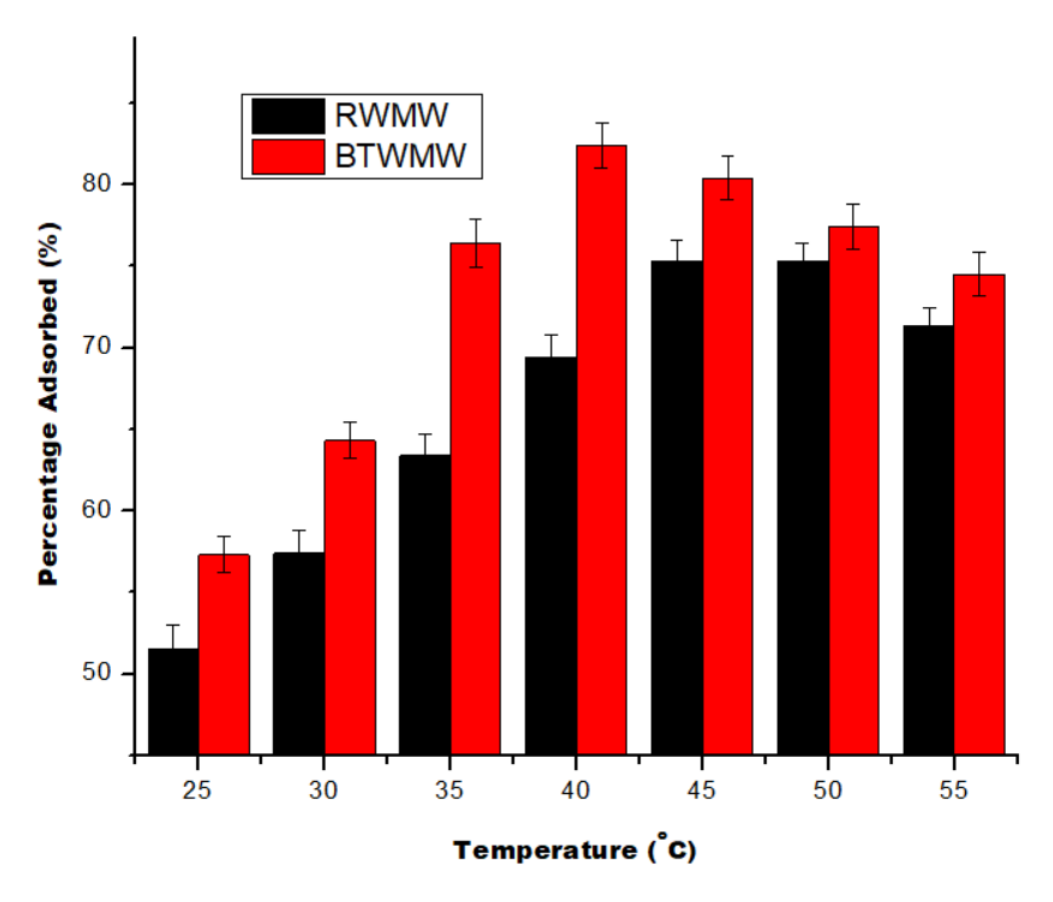


Fig. 10. The plots of temperature effect

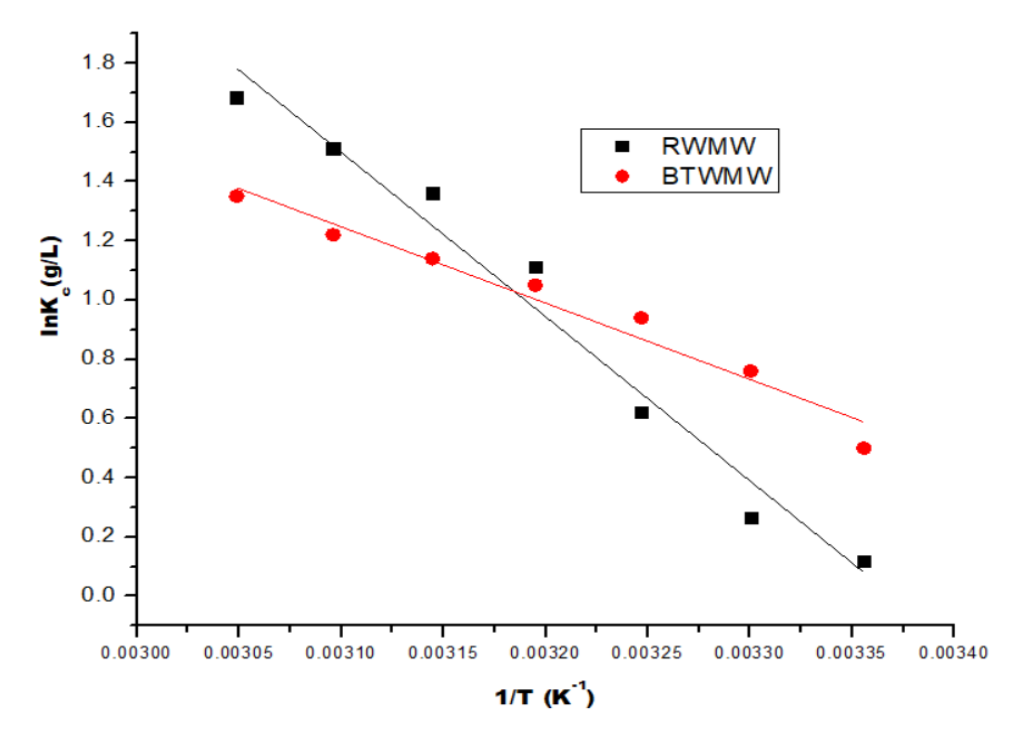


Fig. 11. The plots of thermodynamic

On plotting InK_d against the inverse of temperature, as shown in Fig. 11, the various parameters listed in Table 5 were deduced.

Gibbs Free Energy (ΔG) Analysis

For both RWMW and BTWMW, ΔG values were negative across all temperatures, indicating that the adsorption of MG onto these adsorbents is spontaneous (Oyebola *et al.* 2025). As temperature increased from 25 to 50 °C, ΔG values became more negative, suggesting that the adsorption process was more favorable at higher temperatures. This trend implies an endothermic adsorption process, where increasing temperature enhances dye uptake (Ofudje *et al.* 2024). At 25 °C, the ΔG values for RWMW and BTWMW were -1.32 and -0.85 kJ/mol, respectively, indicating that RWMW initially showed slightly more spontaneous adsorption. However, at higher temperatures (50 °C), ΔG for RWMW reached -2.36 kJ/mol, while that for BTWMW was -2.04 kJ/mol, suggesting that while both adsorbents benefited from increased temperature, the relative Gibbs free energy difference remained relatively stable beyond 298 K.

Enthalpy (ΔH) and Entropy (ΔS) Analysis

The positive ΔH values for both RWMW (17.2 kJ/mol) and BTWMW (21.4 kJ/mol) confirm that the adsorption process was endothermic, meaning that heat is absorbed during dye uptake (Adeogun *et al.* 2018; Oyebola *et al.* 2025). The higher ΔH for BTWMW suggests that the base treatment increased the adsorption affinity, possibly by enhancing functional groups on the surface that interact with malachite green molecules. Based on the FTIR analysis, the functional groups involved in the interaction with malachite green molecules potentially included –OH, –COOH, –NH, C=C, and C-O groups. These groups can facilitate adsorption through hydrogen bonding, and

electrostatic attraction with the aromatic rings of malachite green. Entropy changes (ΔS) were also positive for both adsorbents (6.04 J/mol·K for RWMW and 10.26 J/mol·K for BTWMW), indicating an increase in randomness at the solid-liquid interface during adsorption. The larger ΔS for BTWMW implies that adsorption results in greater disorder, likely due to higher active site availability following base treatment. The study by Konicki *et al.* (2017) observed negative ΔG° values across all temperatures, indicating that the adsorption process is spontaneous. Moreover, the magnitude of ΔG° becomes more negative with increasing temperature, reinforcing that higher temperatures favor the adsorption process. Gupta *et al.* (2010) reported that the adsorption process of Rhodamine-B (RB) dye onto mustard cake (MC) and activated carbon (AC) is spontaneous and endothermic, with higher temperatures enhancing dye uptake.

In a report documented by Hussien-Hamad (2023), it was observed that the adsorption rate of MG by nano-bentonite rose with temperature. It was reported that at 25 °C, the removal percentage was 92.2%, which rose to 99.8% at 35 °C, and the process was said to be endothermic. The study by Konicki *et al.* (2017) examines adsorption at various temperatures and it was noted that when temperature rose from 20 to 60 °C, the uptake of BR46 and BY28 rose from 62.0 to 66.1 mg g⁻¹ and from 48.5 to 53.1 mg g⁻¹, respectively, indicating endothermic process. Gupta *et al.* (2010) observed that while Rhodamine-B uptake by charcoal surged with rising temperature, indicating an endothermic process, that of mustard cake was exothermic, as elevated temperature causes the expansion of the adsorbent's pores, leading to the release of some molecules of the dye from its interior.

Table 5. Thermodynamics Parameters of MG Adsorption by RWMW and BTWMW

	RWMW			BTWMW		
<i>T</i> (K)	ΔG (kJ/mol)	Δ <i>H</i> (kJ/mol)	ΔS (J/mol·K)	ΔG (kJ/mol)	Δ <i>H</i> (kJ/mol)	ΔS (J/mol·K)
298	-1.32			-0.85		
303	-1.43			-1.22		
308	-1.65	17.24	6.04	-1.37	21.44	10.26
313	-1.86			-1.58		
318	-2.03			-1.84		
323	-2.36			-2.04		
328	-1.32			-0.85		

Desorption Study

Desorption studies are crucial in understanding the reusability of an adsorbent and the strength of the interaction between the dye and the adsorbent surface. The data for raw wood mill waste and base-treated wood mill waste revealed the extent to which MG can be released back into the solution by acetic acid treatment over five desorption cycles, as shown in Fig. 12. For the first desorption cycle, the desorption efficiency was relatively high for both RWMW (73.3%) and BTWMW (77.5%), indicating that a significant portion of the adsorbed MG could be removed from the surface. This suggests that physisorption (weak van der Waals interactions) plays a role in the adsorption mechanism, allowing for easy desorption. As the number of cycles increased, desorption efficiency gradually declines. After two cycles, desorption decreased to 70.4% for

RWMW and 75.8% for BTWMW, and after five cycles, the desorption efficiency was lowest, reaching 58.4% for RWMW and 63.8% for BTWMW. Base-treated wood mill waste consistently exhibited higher desorption efficiency compared to RWMW across all cycles. This indicates that base treatment modifies the surface chemistry. The higher desorption efficiency of BTWMW suggests that it can be regenerated more effectively than RWMW, making it a better candidate for reuse in multiple adsorption-desorption cycles. The gradual decrease in desorption efficiency over successive cycles implies that a fraction of MG becomes irreversibly bound to the adsorbent surface. This could be due to chemical interactions, such as complex formation or stronger binding, at specific active sites, particularly after multiple adsorption-desorption cycles.

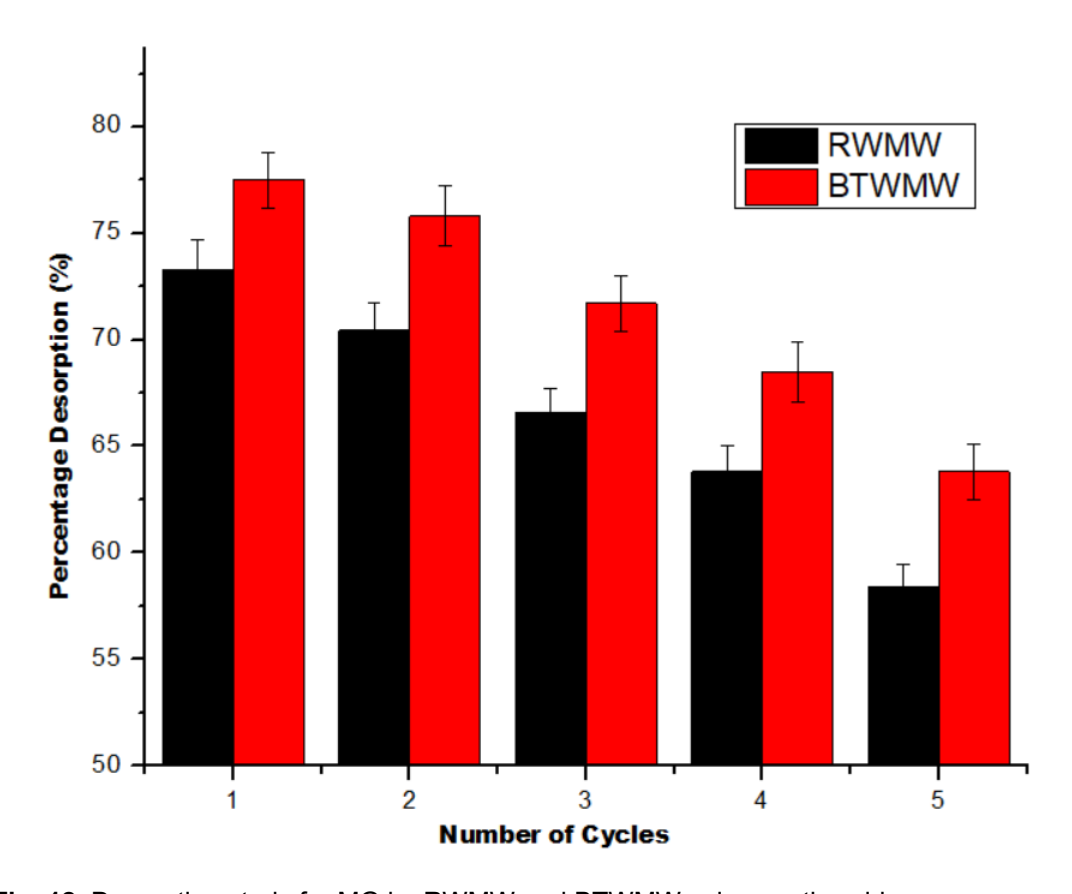


Fig. 12. Desorption study for MG by RWMW and BTWMW using acetic acid

Characterizations

The base treatment of wood mill waste enhanced its physicochemical properties, making it a more effective adsorbent compared to RWMW, as presented in Table 6. The surface area of base-treated wood mill waste BTWMW increased from 73.6 to 114.1 m²/g, indicating increased porosity and a greater number of active sites for adsorption (Henao-Toro *et al.* 2024). Similarly, the pore volume expanded from 0.22 to 0.27 cm³/g, allowing for better retention and interaction with adsorbates. The average pore size also increased from 2.03 nm to 2.66 nm, suggesting that base treatment widens the pores, facilitating better accessibility for pollutants (Henao-Toro *et al.* 2024). Additionally, the bulk density experienced a slight increase from 0.225 to 0.241 g/cm³, which may affect packing efficiency in filtration systems. The pH at the zero point of charge (pHzPC)

shifted slightly from 4.25 to 4.71, indicating changes in surface functional groups that could influence adsorption behavior, particularly for pH-sensitive contaminants. Overall, these modifications demonstrate that base treatment enhanced the adsorption potential of wood mill residue, making BTWMW a more efficient and cost-effective alternative to RWMW.

Parameters	RWMW	BTWMW
Surface area (m²/g)	73.6	114.1
Pore volume (cm²/g)	0.22	0.27
Average pore size (nm)	2.03	2.66
Bulk density (g/cm²)	0.225	0.241
рНирс	4.25	Δ 71

Table 6. Physicochemical Features of RWMW and BTWMW

The FT-IR spectral curves compare the base-modified wood waste before adsorption (a) and after adsorption of malachite green dye (b), as shown in Fig. 13. The changes in functional groups provide insight into the adsorption process and the interaction between the dye molecules and the wood waste surface. In spectrum (a), corresponding to the adsorbent before adsorption, a broad peak appears around 3367 to 3588 cm⁻¹. This is typically attributed to O–H stretching vibrations from hydroxyl groups, which are abundant in lignocellulosic materials like wood waste (Lee *et al.* 2019; Ojediran *et al.* 2021). After MG adsorption (spectrum b), this peak shifted slightly and changed in intensity, suggesting that hydrogen bonding or electrostatic interactions occurred between the adsorbent's surface and the dye molecules.

The region near 3015 to 2980 cm⁻¹, corresponding to C-H stretching vibrations of aliphatic -CH2 groups, remained largely unchanged (Sartape et al. 2017), and this indicates that the hydrocarbon backbone of the adsorbent was not significantly involved in the adsorption process. However, in the region around 1750 to 1695 cm⁻¹, which is typically associated with C=O stretching of carboxylic acids or ketones, noticeable changes are apparent. A particularly important region lies around 1656 to 1540 cm⁻¹, where C=C stretching vibrations of aromatic rings and N-H bending occur. After adsorption, new or intensified peaks in this region suggest the incorporation of MG's aromatic structure, confirming its successful adsorption onto the surface (Lee et al. 201). A study by Ojediran et al. (2021) on the adsorption of MG onto acid-functionalized maize cob reported peaks between 1515.1 and 1427.7 cm⁻¹, and these were attributed to C=C bending of the aromatic ring. These peaks were present before adsorption and exhibited shifts after MG uptake, indicating interactions between MG and the aromatic structures of the adsorbent. Additionally, the C-O stretching vibrations was seen at 1015 cm⁻¹ in spectrum before adsorption, which shifted to 1020 cm⁻¹, and this further supported the successful adsorption of malachite green onto the wood waste. Ojediran et al. (2021) observed a C-O vibrational band at 1049.93 cm⁻¹ in AFMC before adsorption, which showed changes post-adsorption, suggesting the involvement of C-O functional groups in the adsorption process.

Finally, the peaks shown at 952, 885, 755, and 620 cm⁻¹ are generally associated with out-of-plane bending vibrations of C-H in aromatic rings (indicative of lignin) and possibly skeletal vibrations of polysaccharides (cellulose, hemicellulose), reinforcing the

conclusion that MG dye, which has a strong aromatic component, is now present on the adsorbent surface. After adsorption, however, these peaks shifted in positions coupled with slight reductions in intensity indicating interaction with the adsorbate, likely involving lignin, cellulose, or residual inorganic groups in the base-treated wood residue. The FT-IR analysis confirmed that the base-modified wood waste more effectively adsorbed malachite green dye, as evidenced by changes in key functional groups. The main interaction mechanisms involved in the adsorption process may include hydrogen bonding, electrostatic attraction, and π - π interactions, demonstrating that the modified wood waste is a promising material for dye removal applications.

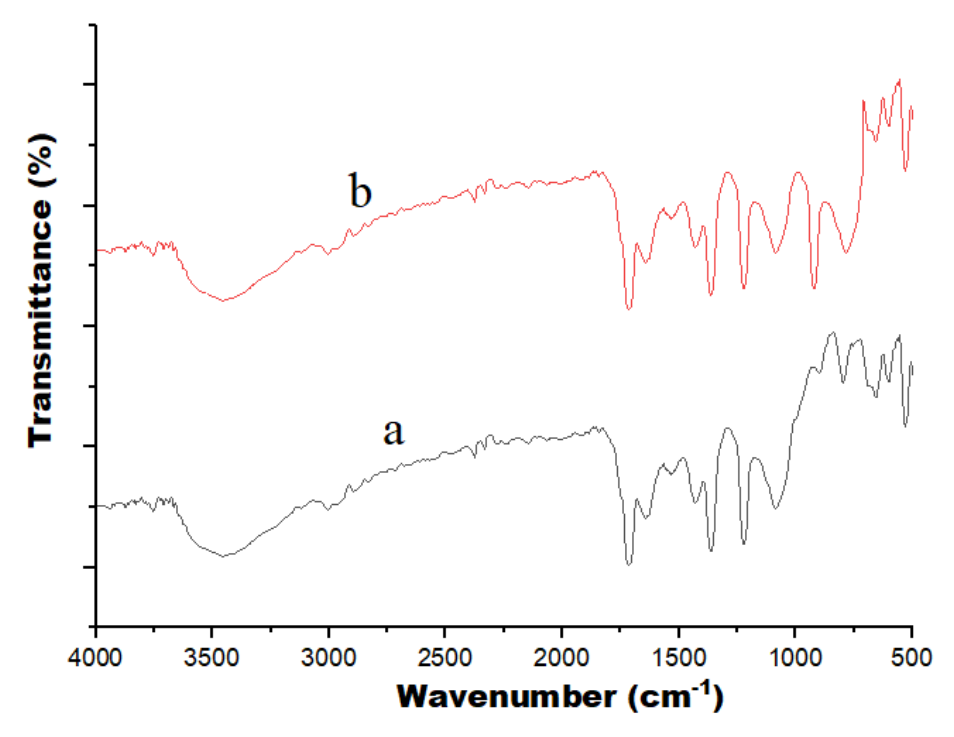


Fig. 13. FT-IR of base-treated wood mill waste before (a) and after (b) the adsorption of MG

The SEM images illustrate the morphological changes in base-modified wood mill residue when comparing before and after adsorption of MG. In Fig. 14(a), taken before adsorption, the surface appears rough and highly porous, with noticeable cavities and irregular textures, indicating a high surface area suitable for adsorption.

The structure is fibrous and well-defined, characteristic of modified lignocellulosic materials. In contrast, Fig. 14(b), taken after adsorption, shows a more compact and less porous surface, with reduced or blocked pores, suggesting successful adsorption of MG molecules. The surface appears more aggregated, likely due to dye deposition, and the reduced roughness indicates that MG has occupied the available adsorption sites.

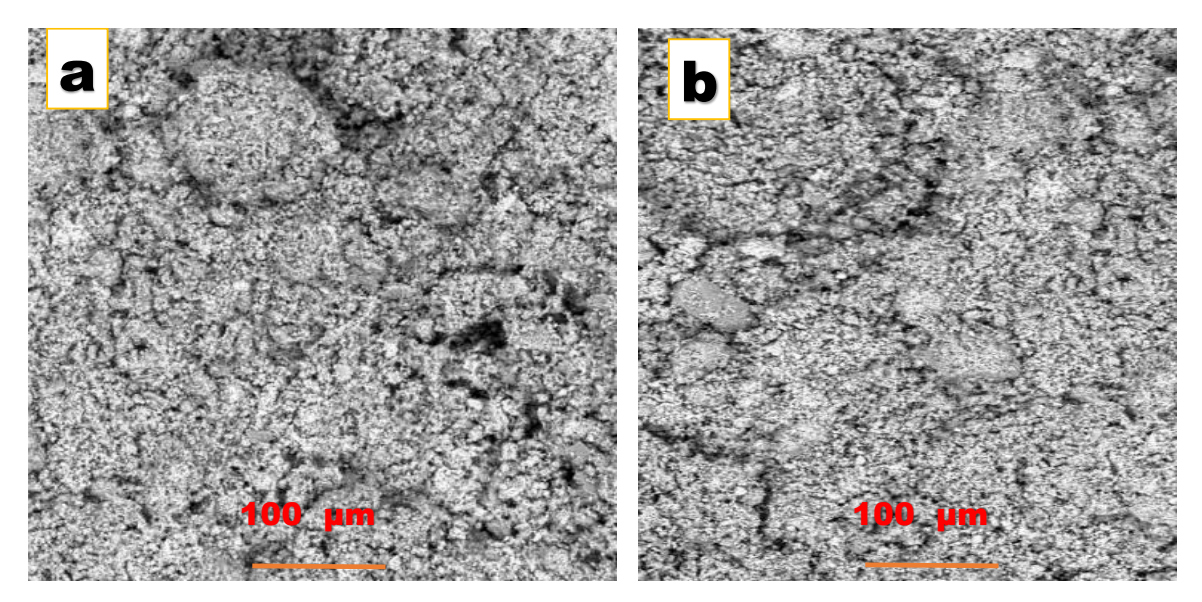


Fig. 14. SEM of base-treated wood mill waste before (a) and after (b) the adsorption of MG

CONCLUSIONS

This study examined the sorption of malachite green (MG) dye using chemically treated wood mill residue in a batch process. The following key deductions were made:

- 1. Base-treated saw mill wood provided better adsorption performance towards MG removal from water.
- 2. The findings demonstrate that factors including temperature, dosage, contact time, and pH influenced the adsorption efficiency.
- 3. An optimum sorption capacity of 44.6 mg/g for the raw sample at 150 min and 55.7 mg/g for the chemically treated sample at 180 min was obtained.
- 4. The process was endothermic, as indicated by positive enthalpy change values.
- 5. The desorption results demonstrated the potential for adsorbent regeneration and reusability, by means of acetic acid treatment, thereby promoting sustainability.
- 6. The FT-IR characterization confirmed successful adsorption of MG by base-modified wood waste, with identified changes in absorbances related to key functional groups

These findings contribute to understanding the adsorption behavior of malachite green and aid in developing effective adsorbents for environmental remediation.

ACKNOWLEDGMENTS

The authors express their appreciation to Northern Border University, Arar, Saudi Arabia, for supporting this work through the project number "NBU-CRP-2025-2985". Furthermore, authors wish to express their appreciation for the financial support *via* Princess Nourah bint Abdulrahman University Researchers Supporting Project number

(PNURSP2025R65), Princess Nourah bint Abdulrahman University, Riyadh, Saudi Arabia.

REFERENCES CITED

- Abewaa, M., Mengistu, A., Takele, T., Fito, J., and Nkambule, T. (2023). "Adsorptive removal of malachite green dye from aqueous solution using *Rumex abyssinicus* derived activated carbon," *Sci. Rep.* 13, article 14701. DOI: 10.1038/s41598-023-41957-x
- Adeogun, A. I., Ofudje, E. A., Idowu, M. A., Kareem, S. O., Vahidhabanu, S., and Babu, B. R. (2018). "Biosorption of Cd²⁺ and Zn²⁺ from aqueous solution using tilapia fish scale (*Oreochromis* sp): Kinetics, isothermal and thermodynamic study," *Desal. Water Treat.* 107, 182-194. DOI: 10.5004/dwt.2018.22122
- Bashanaini, S. M. (2019). "Removal of malachite green dye from aqueous solution by adsorption using modified and unmodified local agriculture waste," *Sci. J. Anal. Chem.* 7(2), 42-56. DOI: 10.11648/j.sjac.20190702.12
- Bayram, O., Köksal, E., Göde, F., and Pehlivan, E. (2022). "Decolorization of water through removal of methylene blue and malachite green on biodegradable magnetic *Bauhinia variagata* fruits," *Int. J. Phytorem.* 24, 311-323. DOI: 10.1080/15226514. 2021.1937931
- Blanchard, G., Maunaye, M., and Martin, G. (1984). "Removal of heavy metals from waters by means of natural zeolites," *Water Res* 18(12), 1501-1507. DOI: 10.1016/0043-1354(84)90124-6
- Cerasella, I., Silvia, B., and Andrada, M. (2017). "Adsorptive removal of malachite green from model aqueous solutions by chemically modified waste green tea biomass," *Acta Chim Slov* 64(2), 513-521. DOI: 10.17344/acsi.2017.3271
- Chowdhury, S., and Saha, P. (2010). "Sea shell powder as a new adsorbent to remove basic green 4 (malachite green) from aqueous solutions: Equilibrium, kinetic and thermodynamic studies," *Chem. Eng. J.* 164, 168-177. DOI: 10.1016/j.cej.2010.08.050
- Deniz, F. (2024). "Cost-efficient and sustainable treatment of malachite green, a model micropollutant with a wide range of uses, from wastewater with *Pyracantha coccinea* M. J. Roemer plant, an effective and eco-friendly biosorbent," *J. Taibah Univ. Sci.* 18(1), article ID 2253592. DOI: 10.1080/16583655.2023.2253592
- Du, B. Y., Wang, Y. M., Zheng, Q., Wang, X., Chen, X. H., Zhou, J. H., Yang, G. H., and Sun, R.-C. (2024). "A novel modified lignin-based adsorbent for removal of malachite green and Pb²⁺ ions from wastewater," *Sep. Purific. Technol.* 330(Part C), article ID 125495. DOI: 10.1016/j.seppur.2023.125495
- El-Rayyes, A., Arogundade, I., Ogundiran, A. A., Hefnawy, M., Ofudje, E. A., El Gamal, A., Albedair, L. A., and Alsuhaibani, A. M. (2025). "Hot water-treated cow waste use as an efficient adsorbent for cresol red dye and chromium VI removal from aqueous solutions," *BioResources* 20(2), 3252-3285. DOI: 10.15376/biores.20.2.3252-3285
- Fatma, S., Hameed, A., Noman, M., and Ahmed, T. (2018). "Lignocellulosic biomass: A sustainable bioenergy source for the future," *Protein Pept. Lett.* 25, 148-163. DOI: 10.2174/0929866525666180122144504.
- Giri, B. S., Sonwani, K. R., Varjani, S., Chaurasia, D., Varadavenkatesan, T., Chaturvedi, P., Yadav, S., Katiyar, V., Singh, R. S., and Pandey, A. (2022). "Highly efficient

- bioadsorption of malachite green using Chinese fan-palm biochar (*Livistona chinensis*)," *Chemosphere* 287, article ID 132282. DOI: 10.1016/j.chemosphere.2021.132282
- Gunduz, F., and Bayrak, B. (2017). "Biosorption of malachite green from an aqueous solution using pomegranate peel: Equilibrium modelling, kinetic and thermodynamic studies," *J. Mol. Liq.* 243, 790-798.
- Gupta, V. K., Jain, R., Siddiqui, M. N., Saleh, T. A., Agarwal, S., Malati, S., and Pathak, D. (2010). "Equilibrium and thermodynamic studies on the adsorption of the dye Rhodamine-B onto mustard cake and activated carbon," *J. Chem. & Eng. Data* 55(11), 5225-5229. DOI: 10.1021/je1007857
- Guruprasad, M. J., Rajesha, G., Shashikanth, Shareefraza, J. U., Shamsuddin A., Majed A., and Saiful, I. (2024). "Studies on the removal of malachite green from its aqueous solution using water-insoluble β-cyclodextrin polymers," *ACS Omega* 9, 10132-10145. DOI: 10.1021/acsomega.3c06504
- Hameed, B. H., and El-Khaiary, M. I. (2008). "Malachite green adsorption by rattan sawdust: Isotherm, kinetic and mechanism modeling," *J. Hazard. Mat.* 159(2-3), 574-579.
- Hasanah, M., Wijaya, A., Arsyad, F. S., Mohadi, R., and Lesbani, A. (2023). "Preparation of C-based magnetic materials from fruit peel and hydrochar using snake fruit (*Salacca zalacca*) peel as adsorbents for the removal of malachite green dye," *Environ. Nat. Resour.* 21, 67-77.
- Henao-Toro H., Juan F. P., and Rubio-Clemente, A. (2024). "Malachite green dye removal in water by using biochar produced from *Pinus patula* pellet gasification in a reverse downdraft reactor," *Sustain*. 16(24), article ID 11043. DOI: 10.3390/su162411043
- Ho, Y. S., and McKay, G. (1999). "Pseudo-second order model for sorption processes," *Process Biochem.* 34(5), 451-465. DOI: 10.1016/S0032-9592(98)00112-5
- Ho, Y. S. (2006). "Second-order kinetic model for the sorption of cadmium onto tree fern: a comparison of linear and nonlinear methods," *Water Res* 40(1), 119-125. DOI: 10.1016/j.watres.2005.10.040
- Hussien-Hamad, M. T. M. (2023). "Optimization study of the adsorption of malachite green removal by MgO nano-composite, nano-bentonite and fungal immobilization on active carbon using response surface methodology and kinetic study," *Environ. Sci. Eur.* 35, article 26. DOI: 10.1186/s12302-023-00728-1
- Jyotshana, S., Shubhangani, S., and Vineet, S. (203). "Toxicity of malachite green on plants and its phytoremediation: A review," *Regional Studies in Marine Science* 62, article ID 102911. DOI: 10.1016/j.rsma.2023.102911
- Konicki, W., Aleksandrzak, M., and Mijowska, E. (2017). "Equilibrium, kinetic and thermodynamic studies on adsorption of cationic dyes from aqueous solutions using graphene oxide," *Chem. Eng. Res. Des.* 123, 35-49. DOI: 10.1016/j.cherd.2017.03.036
- Lagergren, S. K. (1898). "About the theory of so-called adsorption of soluble substances," *Sven Vetenskapsakad Handingarl* 24, 1-39.
- Lee, S. L., Park, J. H., Kim, S. H., Kang, S-W., Cho, J-S., Jeon, J-R., Lee, Y-B., and Seo, D-C. (2019). "Sorption behavior of malachite green onto pristine lignin to evaluate the possibility as a dye adsorbent by lignin," *Appl. Biol. Chem.* 62, article 37. DOI: 10.1186/s13765-019-0444-2

- Muinde, V. M., Onyari, J. M., Wamalwa, B., Wabomba, J., and Nthumbi, R. M. (2017). "Adsorption of malachite green from aqueous solutions onto rice husks: Kinetic and equilibrium studies," *J. Environ. Prot.* 8, 215-230. DOI: 10.4236/jep.2017.83017
- Negeno, E, C., Mbuci, K. E., Necibi, M. C., Shikuku, V. O., Olisah, C., Ongulu, R., Matovu, H., Ssebugere, P., Abushaban, A., and Sillanpaa, M. (2022). "Sustainable reutilization of waste materials as adsorbents for water and wastewater treatment in Africa: Recent studies, research gaps, and way forward for emerging economies," *Environ. Adv.* 9, article ID 100282. DOI: 10.1016/j.envadv.2022.100282
- Ofudje, E. A., Al-Ahmary, K. M., Alzahrani, E. A., Ud Din, S., and Al-Otaibi, J. S. (2024). "Sugarcane peel ash as a sorbent for methylene blue," *BioResources* 19(4), 9191-9219. DOI: 10.15376/biores.19.4.9191-9219
- Ofudje, E. A., Adeogun, A. I., Idowu, M. A., Kareem, S. O., and Ndukwe, N. A. (2020). "Simultaneous removals of cadmium(II) ions and reactive yellow 4 dye from aqueous solution by bone meal-derived apatite: Kinetics, equilibrium and thermodynamic evaluations," *J. Anal. Sci. Technol.* 11, article 7. DOI: 10.1186/s40543-020-0206-0
- Ojediran, J. O., Dada, A. O., Aniyi, S. O., David, R. O., and Adewumi, A. D. (2021). "Mechanism and isotherm modeling of effective adsorption of malachite green as endocrine disruptive dye using acid functionalized maize cob (AFMC)," *Sci. Rep.* 11, article 21498. DOI: 10.1038/s41598-021-00993-1
- Oyebola, E. O., Hefnawy, M., Ofudje, E. A., El Gamal, A., Akande, J. A., and Emran, T. B. (2025). "Nickel ions biosorption onto sawmill wood waste products: Kinetics, equilibrium, and thermodynamic investigations," *BioResources* 20(2), 3024-3046. DOI: 10.15376/biores.20.2.3024-3046
- Oyelude, E. O., Awudza, J. A. M., and Twumasi, S. K. (2018). "Removal of malachite green from aqueous solution using pulverized teak leaf litter: Equilibrium, kinetic and thermodynamic studies," *Chem. Centr. J.* 12, article 81. DOI: 10.1186/s13065-018-0448-8
- Parimelazhagan, V., Yashwath, P., Arukkani Pushparajan, D., and Carpenter, J. (2022). "Rapid removal of toxic Remazol Bril liant Blue-R dye from aqueous solutions using *Juglans nigra* shell biomass activated carbon as potential adsorbent: Optimization, isotherm, kinetic, and thermodynamic investigation," *Int. J. Mol. Sci.* 23(20), article 12484. DOI: 10.3390/ijms232012484
- Pehlivan, M., Simsek, S., Ozbek, S., and Ozbek, B. (2020). "An optimization study on adsorption of Reactive Blue 19 dye from aqueous solutions by extremely effective and reusable novel magnetic nanoadsorbent," *Desal. Water Treat.* 191, 438-451. DOI: 10.5004/dwt.2020.25753
- Rangabhashiyam, S., and Balasubramanian, P. (2018). "Performance of novel biosorbents prepared using native and NaOH treated *Peltophorum pterocarpum* fruit shells for the removal of malachite green," *Bioresource Technology Reports*, DOI: 10.1016/j.biteb.2018.06.004
- Sartape, A. S., Mandhare, A. M., Jadhav, V. V., Raut, P. D., Anuse M. A., and Kolekar, S. S. (2017). "Removal of malachite green dye from aqueous solution with adsorption technique using *Limonia acidissima* (wood apple) shell as low cost adsorbent," *Arabian J. Chem.* 10(2), S3229-S3238. DOI: 10.1016/j.arabjc.2013.12.019
- Shanmugarajah, B., Chew, I. M., Mubarak, N. M., Choong, T. S., Yoo, C., and Tan, K. (2018). "Valorization of palm oil agro-waste into cellulose biosorbents for highly effective textile effluent remediation," *J. Clean. Prod.* 210, 697-709. DOI: 10.1016/j.jclepro.2018.10.342

- Singh, V., Soni, A., and Singh, R. (2016). "Process optimization studies of malachite green dye adsorption onto *Eucalyptus (Eucalyptus globulus*) wood biochar using response surface methodology," *Oriental J. Chem.* 32(5), 2621-2631. DOI: 10.13005/ojc/320534
- Srivastava, S., Sinha, R., and Roy, D. (2004). "Toxicological effects of malachite green," *Aquatic Toxicol.* 66(3), 319-329. DOI: 10.1016/j.aquatox.2003.09.008
- Sugiarto, S., Pong, R. R., Tan, Y. C., and Leow, Y. (2022). "Advances in sustainable polymeric materials from lignocellulosic biomass," *Mater. Today* 26, article 101022. DOI: 10.1016/j.mtchem.2022.101022
- Tsoutsa, E. K., Tolkou, A. K., Kyzas, G. Z., and Ioannis, A. K. (2024). "An update on agricultural wastes used as natural adsorbents or coagulants in single or combined systems for the removal of dyes from wastewater," *Water Air Soil Poll.* 235, article 178. DOI: 10.1007/s11270-024-06979-9
- Velinov, N., Miljana, R. V. M., Jerman, I., Markovic, N. D., Nikolic, G., Bojic, D., and Bojic, A. (2024). "The application of wood biowaste chemically modified by Bi₂O₃ as an adsorbent material for wastewater treatment," *Processes* 12, article 2025. DOI: 10.3390/pr12092025
- Yıldız, D., Demir, I. and Demiral H. (2023). "Adsorption of malachite green on to poplar sawdust activated carbon," *Sep. Sci. Technol.* 58(12), 2099-2114. DOI: 10.1080/01496395.2023.2240492

Article submitted: April 2, 2025; Peer review completed: May 15, 2025; Revised version received: May 20, 2025; Accepted: June 9, 2025; Published: July 21, 2025. DOI: 10.15376/biores.20.3.7378-7404